# BRAIN
A JOURNAL OF NEUROLOGY

# Brain catecholamine depletion and motor impairment in a *Th* knock-in mouse with type B tyrosine hydroxylase deficiency

Germaine Korner,[1,2,3,*] Daniela Noain,[4,*] Ming Ying,[5] Magnus Hole,[5] Marte I. Flydal,[5]
Tanja Scherer,[1,3] Gabriella Allegri,[1,3] Anahita Rassi,[6] Ralph Fingerhut,[7,3]
Damasia Becu-Villalobos,[8] Samyuktha Pillai,[9] Stephan Wueest,[3,10] Daniel Konrad,[3,10]
Anna Lauber-Biason,[11] Christian R. Baumann,[2,4] Laurence A. Bindoff,[12,13] Aurora Martinez[5]
and Beat Thöny[1,2,3]

*These authors contributed equally to this work.

Tyrosine hydroxylase catalyses the hydroxylation of L-tyrosine to L-DOPA, the rate-limiting step in the synthesis of catecholamines. Mutations in the *TH* gene encoding tyrosine hydroxylase are associated with the autosomal recessive disorder tyrosine hydroxylase deficiency, which manifests phenotypes varying from infantile parkinsonism and DOPA-responsive dystonia, also termed type A, to complex encephalopathy with perinatal onset, termed type B. We generated homozygous *Th* knock-in mice with the mutation *Th*-p.R203H, equivalent to the most recurrent human mutation associated with type B tyrosine hydroxylase deficiency (*TH*-p.R233H), often unresponsive to L-DOPA treatment. The *Th* knock-in mice showed normal survival and food intake, but hypotension, hypokinesia, reduced motor coordination, wide-based gate and catalepsy. This phenotype was associated with a gradual loss of central catecholamines and the serious manifestations of motor impairment presented diurnal fluctuation but did not improve with standard L-DOPA treatment. The mutant tyrosine hydroxylase enzyme was unstable and exhibited deficient stabilization by catecholamines, leading to decline of brain tyrosine hydroxylase-immunoreactivity in the *Th* knock-in mice. In fact the substantia nigra presented an almost normal level of mutant tyrosine hydroxylase protein but distinct absence of the enzyme was observed in the striatum, indicating a mutation-associated mislocalization of tyrosine hydroxylase in the nigrostriatal pathway. This hypomorphic mouse model thus provides understanding on pathomechanisms in type B tyrosine hydroxylase deficiency and a platform for the evaluation of novel therapeutics for movement disorders with loss of dopaminergic input to the striatum.

1 Division of Metabolism, Department of Paediatrics, University of Zürich, Zürich, Switzerland
2 Affiliated with the Neuroscience Centre Zurich ZNZ, Zürich, Switzerland
3 Affiliated with the Children's Research Centre CRC, Zürich, Switzerland
4 Department of Neurology, University Hospital of Zurich, Zürich, Switzerland
5 Department of Biomedicine, University of Bergen, Bergen, Norway
6 Division of Clinical Chemistry and Biochemistry, Department of Paediatrics, University of Zürich, Zürich, Switzerland
7 Swiss Newborn Screening Laboratory, University Children's Hospital, Zurich, Switzerland
8 Institute of Biology and Experimental Medicine, Buenos Aires, Argentina
9 Institute of Physiology, University of Zurich, Zürich, Switzerland
10 Division of Endocrinology, Department of Pediatrics, University of Zurich, Switzerland
11 Department of Medicine, University of Fribourg, Fribourg, Switzerland
12 Department of Clinical Medicine K1, University of Bergen, Norway
13 Department of Neurology, Haukeland University Hospital, Bergen, Norway

Correspondence to: Dr Aurora Martinez,
Department of Biomedicine,
University of Bergen, Jonas Lies vei 91,
5009 Bergen, Norway
E-mail: aurora.martinez@biomed.uib.no

Correspondence may also be addressed to: Dr Beat Thöny,
Division of Metabolism,
Department of Pediatrics,
University of Zurich, Steinwiesstrasse 75,
CH-8032 Zürich, Switzerland
E-mail: beat.thony@kispi.uzh.ch

# Introduction

Tyrosine hydroxylase (TH; EC 1.14.16.2) is a homotetrameric enzyme that catalyses the conversion of L-tyrosine to L-dihydroxyphenylalanine (L-DOPA) by using molecular oxygen as additional substrate and the cofactor (6R)-L-erythro-5,6,7,8-tetrahydrobiopterin ($BH_4$) (Nagatsu et al., 1964; Roberts and Fitzpatrick, 2013). This hydroxylation is the rate-limiting step in the synthesis of the catecholamine neurotransmitters dopamine, norepinephrine and epinephrine (Nagatsu et al., 1964). Dopamine is distinctively involved in motor control, but also in cognition, memory and reward and, as a precursor of norepinephrine and epinephrine, indirectly regulates attention and helps to maintain normal blood pressure and blood sugar (Eisenhofer et al., 2004). In the CNS, TH is mainly expressed in dopaminergic neurons of the substantia nigra, which project mostly to the striatum and have a central role in motor control, and in the ventral tegmental area, which projects to the nucleus accumbens and the prefrontal cortex and regulates motivation and reward. TH is also expressed in noradrenergic neurons of the locus coeruleus and lateral tegmental system (Zigmond et al., 1989; Bjorklund and Dunnett, 2007). Outside the CNS, TH expression is found in the adrenal medulla, the sympathetic neurons, and in non-neuronal (renal, intestine, pancreatic and lymphoid) tissues. The single human TH gene undergoes alternative mRNA splicing generating four main isoforms (hTH1–hTH4), with variations in the length of the N-terminal, where hTH4 corresponds to the longest, full-length isoform and hTH1 to the shortest and most abundant one, equivalent to rodent TH (Nagatsu, 1995). TH activity is tightly controlled by regulatory mechanisms at the transcriptional, translational and post-translational levels (Kumer and Vrana, 1996; Tank et al., 2008). The latter includes phosphorylation at several Ser/Thr residues at the N-terminal tail (Daubner et al., 2011). Notably, phosphorylation at Ser40 by cAMP-dependent protein kinase A activates TH by releasing the feedback inhibition of catecholamines and decreasing the $K_m$ for the cofactor $BH_4$ (Nagatsu et al., 1964). Binding of the catecholamine end-products inactivates and stabilizes TH both in vitro (Okuno and Fujisawa, 1991; Martinez et al., 1996) and in vivo (Sumi-Ichinose et al., 2001). Another short-term regulatory mechanism of TH of important biological significance is substrate inhibition, that allows steady synthesis of dopamine despite fluctuations in blood L-tyrosine (Reed et al., 2010).

Mutations in the TH gene (OMIM *191290) cause TH deficiency (THD; OMIM #605407), which is a rare disorder that comprises a broad phenotypic variation including infantile parkinsonism and L-DOPA-responsive dystonia (DRD). THD manifestations range from a mild progressive limb dystonia, postural tremor and hypokinetic rigid syndrome that is responsive to L-DOPA (termed type A) to a progressive and complex neonatal or early-infancy onset encephalopathy with L-DOPA-unresponsive parkinsonism (termed type B) (Willemsen et al., 2010). A certain genotype–phenotype correlation between the clinical subtype and the genotype of the THD patients through the in vitro TH activity of the mutant variants has recently been reported (Fossbakk et al., 2014). Nevertheless, an accurate clinical diagnosis of THD must be based on central catecholamine deficiency reflected by normal 5-hydroxyindolacetic acid (5-HIAA) but low homovanillic acid (HVA), low 3-methoxy-4-hydroxyphenylethylene glycol (MHPG) and low HVA:5-HIAA ratio in CSF from lumbar puncture (Willemsen et al., 2010), and by mutation analysis of the TH gene (Haavik et al., 2008; Kurian et al., 2011). Peripheral (urinary) concentration of catecholamines, HVA and MHPG are non-informative most probably due to dopamine production by residual TH and tyrosinase activity in non-neuronal tissues (Willemsen et al., 2010). Elevated serum prolactin may, however, be used as a peripheral biomarker reflecting central neurotransmitter status (Aitkenhead and Heales, 2013).

The release of this hormone from the pituitary gland is under control of hypothalamic dopamine, which is the primary physiological inhibitor of prolactin secretion (Ben-Jonathan, 1985). Furthermore, galactorrhoea has been observed in some severely affected hyperprolactinaemic patients with THD (Yeung *et al.*, 2006). To date, ~70 THD patients have been reported (www.biopku.org/pnddb) (Willemsen *et al.*, 2010; Fossbakk *et al.*, 2014); the most recurrent *TH* mutation, accounting for ~30% of all mutant alleles, is c.698G > A/p.Arg233His in exon 6; NM_1999292.2 (corresponding to c.605G > A/ p.Arg202His in hTH1). While as a homozygous or compound heterozygous allele this mutation can be associated with type A or type B THD (Haavik *et al.*, 2008; Willemsen *et al.*, 2010), about half of the patients with type B THD are homozygous for variant p.R233H (Willemsen *et al.*, 2010).

Parkinsonian syndromes, dystonias, and related movement disorders showing a reduction in the levels of TH activity and dopamine levels are closely associated with THD (Kurian *et al.*, 2011; Garcia-Cazorla and Duarte, 2014). Although THD is not accompanied by neurodegeneration, it shares several traits with Parkinson's disease where the motor features actually reflect the loss of striatal dopamine due to degeneration of dopaminergic neurons in the midbrain (Obeso *et al.*, 2010). Transgenic mouse models aiming to mimic THD by inactivating the *Th* gene have been generated in the past (Kobayashi *et al.*, 1995; Zhou *et al.*, 1995; Szczypka *et al.*, 1999). The complete *Th* knock-out was non-viable, and none of the rescue mutants fully reproduced the clinical and pathological features of THD. They did, however, provide valuable insights into the importance of dopamine and the other catecholamines for mouse foetal development (Kobayashi *et al.*, 1995; Zhou *et al.*, 1995) and the functional interdependence of the adrenomedullary and adrenocortical systems (Bornstein *et al.*, 2000).

To provide novel insights into catecholamine function and study the pathophysiological mechanisms responsible for the severe (type B) THD phenotype, we generated a constitutive *Th* knock-in mouse with the p.Arg203His mutation, equivalent to the human *TH*-p.R233H (hTH1-p.R202H). This mouse, here termed *Th* knock-in, was viable and presented with motor dysfunction due to a reduced TH activity and gradual loss of catecholamine metabolites, including dopamine. Measurements in brain extracts, immunohistochemical analyses and kinetic and molecular studies of wild-type and mutant human and mouse enzymes showed the instability of the mutant TH. Importantly, the mutant enzymes could not be stabilized by dopamine, highlighting the importance of a functional regulatory feedback inhibition by catecholamines to maintain TH levels and proper localization. Furthermore, the *Th* knock-in mouse displays the salient clinical features of human type B THD phenotype including biochemical markers, impaired motor function, diurnal fluctuation of symptoms and non-responsiveness to L-DOPA treatment, and

thus represents an ideal model for pathomechanistic studies and for investigations of novel therapeutic approaches, such as pharmacological chaperones and treatment strategies based on circadian regulation of TH activity and/or restorative properties of sleep.

# Materials and methods

## Generation of the *Th* knock-in mouse allele

A C57BL/6 mouse carrying a constitutive knock-in of the point mutation p.Arg203His in the *Th* gene was custom generated by TaconicArtemis (NCBI gene ID 21823, transcript variant *Th*-1 NM_0093771.1; Ensembl gene ID ENSMUSG00000000214). Details on the targeting vector for electroporation, homologous recombination and selection in mouse embryonic stem cells (Art B6/3.6 background C57BL/6 NTac) are given in Supplementary Fig. 1A–C. Validation of correct and single targeting was done by Southern blot and PCR analyses (details on request). For elimination of the *NeoR* cassette, mice were crossed with a FLP-deleter strain [C57BL/6-*Tg*(CAG-*Flpe*)1 Arte] for random integration of the CAGGS-FLPe transgene, and subsequently mice were crossed to homozygosity.

## Genotyping of *Th* knock-in mice

One primer set was used for testing for the presence of an additional 85 bp FRT sequence by fragment size analysis (primers 'For' 4601_33: 5'-GAGCTCCCAGAATTGACAGC-3'; 'Rev' 4601_34: 5'-GATCACACTCCACCATATCAAGG-3') and another set for the presence of the R203H mutation via Sanger sequencing (primers 4602_35: 5'-TGTCAGAGTTGGA TAAGTGTCACC-3' and 4602_36: 5'-TGACAGCTAACCA GTCACCTCC-3'; see also Supplementary Fig. 1B and C). Standard PCR conditions were used for DNA amplification.

## Mouse husbandry and treatment studies

Animal experiments were performed in accordance with the guidelines and policies of the Veterinary Office of the State of Zurich and Swiss law on animal protection, the Swiss Federal Act on Animal Protection (1978), and the Swiss Animal Protection Ordinance (1981). Animal studies received approval from the Cantonal Veterinary Office, Zurich, and the Cantonal Committee for Animal Experiments, Zurich, Switzerland. All mice are generated by back-crossing with C57BL/6J from the Jackson Laboratory (i.e. C57BL/6J, α-synuclein positive), and for controls, we exclusively used the wild-type littermates. Mice were maintained in a humidity and temperature (21–23°C) controlled environment under a 12-h dark–light cycle. For treatment studies, six tablets containing L-DOPA (levodopa 100 mg) and the decarboxylase inhibitor carbidopa (25 mg) were purchased (Sinemet) and diluted in 20 ml of double distilled $H_2O$. For validation, the final concentration of L-DOPA was determined by high performance liquid chromatography (Blau *et al.*, 1999). Newborn

homozygous *Th* knock-in and wild-type control mice were fed for the chronic experiments daily *per os* with a solution containing 10 mg levodopa plus 2.5 mg carbidopa per kg of body weight and per day for a time period of up to 3 weeks of age. Elevation of brain 3-OMD (3-O-methyldopa) and HVA control supported that mice received adequate doses of L-DOPA (Fig. 7). Treated mice were tested 24 h after the last administration for motor behaviour, and at sacrifice, tissue was collected for biochemical analyses. Mock control, independent groups of *Th* knock-in and wild-type mice, sex and age-matched, were given double distilled $H_2O$ in parallel. For the acute L-DOPA treatment experiment, a group of *Th* knock-in plus wild-type control mice were first mock fed and tested for motor function (rotarod and bar test; see below). Following a resting phase of 2–3 h, all mice were loaded *per os* with a single bolus of a solution containing 10 mg levodopa plus 2.5 mg carbidopa per kg of body weight, before retesting these mice for motor coordination within 20–45 min after the L-DOPA loading.

## Metabolic cage analysis

Locomotion, food and water intake, $O_2$ consumption and $CO_2$ production were determined for single housed mice (females at the age of 9 months) during a 24-h period in metabolic cages in an open-circuit indirect calorimetry system as previously described (Wueest *et al.*, 2014) (PhenoMaster, TSE Systems). After being adapted to single caging, mice were placed in cages closed with air-tight lids. Water bottles and food cups were placed on scales to measure water and food intake continuously. The measurements were saved on a computer in 20-min intervals and were used to calculate cumulative food and water intake. Activity data were measured using an infrared light-beam. To measure energy expenditure and respiratory exchange ratio (RER), ambient air was pumped through the cage via a flow controller. Air entering and leaving each cage was monitored for its $O_2$ and $CO_2$ concentration. The cages were connected to two analysers measuring $O_2/CO_2$ concentration of each cage for a period of 2 min in 20-min intervals. Energy expenditure and respiratory exchange ratio were calculated using the manufacturer's software based on the following equation:

$$\text{energy expenditure (kcal/h)} = \frac{3.941 \times VO_2 + 1.106 \times VCO_2}{1000};$$

$$\text{respiratory exchange ratio} = \frac{VCO_2}{VO_2}.$$

## Behavioural motor testing

Experiments were carried out during the light phase, between 10 am and 5 pm, and always at the same time of the day within the same group of animals. Experimental batches were acclimated to the test room for at least 1–2 days before testing.

## Open field test

For the open field test (Bello *et al.*, 2011), Plexiglas activity boxes monitored by a video tracking system (Ethovision, Noldus) were used to assess total horizontal activity and mean velocity of locomotion. Animals were placed in a neutral position of the acrylic boxes ($40 \times 40 \times 46$ cm) and left to explore freely and undisturbed for 30 min. Boxes were carefully cleaned between tests to minimize odour cues in the arena.

## Bar test

For the Bar test (Noain *et al.*, 2013), spontaneous catalepsy was determined in *Th* wild-type and *Th* knock-in mice using the horizontal bar test in which the time of immobility (defined as immobile trunk and limbs) was assessed as described previously. Briefly, to discard the possibility of confounding freezing behaviour induced by fear/stress with catalepsy, all mice were habituated to the experimental context by 2 min free exploration over the working bench and experimental setup. Following this, mice were restrained by the tail, their front paws placed over the 5-cm elevated bar (1-cm diameter, plexiglas) and the back limbs set over the working bench. Immediately after, the timer was started. A trail was considered valid when the animal remained grabbing the bar with the front paws until the timer was running ($\sim$2 s). Usually, 2–4 trials were invalid for each mouse at the beginning of the testing session. The highest immobility score out of five valid trials was considered for the analysis of both wild-type and knock-in subjects. The cut-off of the experiment was set at 180 s.

## Rotarod test

For the Rotarod test (Avale *et al.*, 2004), wild-type and *Th* knock-in mice were individually placed in a neutral position on the immobile rotarod treadmill (UgoBasile). Immediately, the speed was increased to 16 rpm and each mouse was given a 10-min training session. During the training session mice were repositioned on the rod after each fall. Mice were tested 3 h later for 3 min at a fixed velocity of 16 rpm, and the latency to the first fall was recorded for each subject.

## Gait analysis

For gait analysis (de Medinaceli *et al.*, 1982; Kunkel-Bagden *et al.*, 1993; Suresh Babu *et al.*, 2012), both hind and fore paws of mice were inked with non-toxic blue and red ink. Animals were immediately placed at one end of a 30-cm acrylic alley, whose floor was covered in white absorbent paper, and encouraged to walk to the opposite end. The paper was then removed and labelled with the animal ID number for further analysis. The stride length and width were manually measured and normalized to body weight ('size') of each mouse to obtain short-step and wide-based gait indices, respectively.

## Preparation of whole brain lysates from mice

Immediately after sacrifice, whole brains were resected and shock frozen in liquid nitrogen. Frozen brains were grinded to powder under liquid nitrogen; thereafter, all procedures were carried out at 4°C. Powdered brains were 'dissolved' in 1 ml of homogenization buffer containing 50 mM Tris-HCl, pH 7.5, 100 mM KCl, 1 mM dithiothreitol (DTT), 0.2 mM PMSF (stock 10 mg/ml in isopropanol), 1 µM leupeptin

(stock 5 mg/ml in H₂O) and 1 µM pepstatin (stock 1 mg/ml in methanol). A TissueLyser II (Qiagen; cat. no. 85300) was used for preparation of lysate following the manufacturer's protocol.

## Gene (mRNA) expression studies

Total RNA was extracted from powdered mouse brains by the QIAmp RNA Blood Mini Kit (Ref. 52304; Hombrechtikon) and cDNA was produced by the Promega reverse transcription system (Ref. nr. A3500). Mouse *Th*, *Tph1, Tph2* and *Igf1* mRNA expression levels were performed using the commercially available ABI assays (Mm.00447546 for *Th* mRNA; NCBI RefSeq NM_009377.1; Mm00493798_m1 for *Tph*1 mRNA, NCBI RefSeq NM_001136084.1; NM 009414.2; Mm00557717_m1 for *Tph*2 mRNA, NCBI RefSeq NM_173391.2; Mm00439560_m1 for *Igf1\* mRNA, NCBI RefSeq NM_001111274.1). The murine glyceraldehyde-3-phosphate dehydrogenase (*Gapdh*) mRNA (ABI assay ID: Mm99999915_g1; NCBI RefSeq NM_008084.2) was used to normalize the relative *Th*, *Thp1, and Thp2* mRNA levels. Values were calculated as described (Livak and Schmittgen, 2001).

## Determination of protein, neopterin, biopterin and monoamine neuro-transmitter metabolites

Protein concentration (in g/l) was determined by using the M-TP Mikroprotein kit from Beckman Coulter Synchron LX-System (Beckman Coulter Inc; kit-no. 445860). Biopterin, neopterin and monoamine neurotransmitter metabolites were determined in brain tissue following published protocols (Blau *et al.*, 1999; Elzaouk *et al.*, 2003).

## Total thyroxine, thyroid stimulating hormone and prolactin

Serum IGF1 was determined by radioimmunoassay (RIA) using a rat IGF1 RIA kit (DSL-2900, Bühlmann Laboratories) (Elzaouk *et al.*, 2003), total thyroxine from whole blood dried on filter paper was measured with the 'GSP^{TM} Neonatal Thyroxine kit' from PerkinElmer (Life and Analytical Sciences), serum prolactin was quantified using an ELISA kit for mouse and rat (GenWay Biotech, Inc), and glucose was measured according to standard methods on a routine Clinical Chemistry unit on a Beckman Coulter UniCel® DxC 600 (Nyon) following the manufacturer's instructions.

## Measuring blood pressure in mice

A non-invasive computerized tail-cuff system for measuring systolic blood pressure in mice was applied as described (Krege *et al.*, 1995).

## Tissue preparation and immunohistochemistry

Adult mice at the age of 6–7 months were anaesthetized with sodium pentobarbital and, after exsanguination, transcardially perfused with 4% paraformaldehyde in phosphate-buffered saline (PBS, pH 7.4). Brains were immediately removed, post-fixed, cryoprotected in sucrose ladder and stored at −80 °C until further use. For free-floating immunohistochemistry, brains were cryostat sectioned in 40 µm slices, incubated for 1 h in 1% H₂O₂ and then washed. A rabbit polyclonal anti-TH antiserum was used (1:1000; Millipore, AB152) for specific immunostainings of TH cells. Sections were incubated with primary antibody overnight at 4°C together with 2% normal goat serum. After washing, sections were incubated for 2 h at room temperature with a solution containing biotinylated goat anti-rabbit IgG (1:400, Vector Laboratories). After washing, sections were incubated for 1 h at room temperature with avidin/biotin complex (1:200, ABC Vectastain Elite Kit, Vector) and washed twice. Finally, sections were exposed to a solution of 0.025% diaminobenzidine, 0.05% H₂O₂ in Tris-buffered saline buffer and monitored for colour development under a microscope (Gelman *et al.*, 2003).

Congo red staining was performed over *Th* wild-type and *Th* knock-in brain tissue to determine the presence of amyloid deposits indicative of a neurodegenerative process (Bohnen and Jahn, 2013; Catafau and Bullich, 2015). Briefly, we mounted 40-µm cryostat sections and dried them overnight. A 5-min wash in deionized water was followed by 20 min in alkaline sodium chloride solution and 20 min in Alkaline Congo red solution (Sigma-Aldrich, Cat# HT60). We then dehydrated the stained tissue in absolute ethanol and xylene, and finally mounted them for bright field microscopy. We counted TH-positive cell bodies in the midbrain using a semiquantitative method. Briefly, substantia nigra pars compacta/ventral tegmental area sections from two *Th* wild-type and two *Th* knock-in were randomly selected from a pull of stained tissue. Similar anatomical levels were included from each genotype, to avoid misrepresentation. All positive TH cell bodies were counted in one hemi-section from each animal.

Additional methodological information is available in the online Supplementary material.

# Results

## *Th* knock-in mice display moderate growth retardation and hypotension

A constitutive knock-in containing the *Th*-p.Arg203His was generated by homologous recombination in the C57BL/6 background and bred to homozygosity (Supplementary Fig. 1 and Supplementary Table 1). The *Th* knock-in litter size was normal with an expected Mendelian ratio and an apparently normal phenotype initially. After weaning, however, *Th* knock-in mice exhibited moderate and continuous growth retardation with 25–34% less body weight compared to their wild-type or heterozygous littermates (Fig. 1A and B). That this was not due to feeding abnormalities was confirmed quantitatively by metabolic cage analyses showing normal food intake and respiratory exchange ratio. Locomotor activity and energy expenditure were, however, reduced (Supplementary Fig. 2). Follow-up examinations of mutant mice revealed no

constipation, and a quantitative analysis of the fat and total energy contents in faeces also revealed no differences between wild-type and *Th* knock-in mice, indicating that mutant mice had normal absorption and digestion (data not shown). *Th* knock-in was normoglycaemic and *Igf1* gene expression was normal (mRNA of whole brain extracts; not shown) as were IGF1 serum levels in adult mice at the age of 12 weeks (Supplementary Fig. 3A). We noticed however that *Igf1* mRNA was significantly elevated in whole brain extracts from *Th* knock-in mice at the age of 3 weeks (not shown), implying that the IGF system might be involved in brain growth, as suggested by others (Delafontaine *et al.*, 2004). We further detected elevation of the total thyroid hormone thyroxine (Supplementary Fig. 3B) and hypotension (Supplementary Fig. 3C) while serum thyroid stimulating hormone was not different between mutant and control mice (not shown).

Both low body weight and reduced blood pressure are found in patients with type B THD (Grattan-Smith *et al.*, 2002; Willemsen *et al.*, 2010) and in mice with norepinephrine and epinephrine deficiency (Swoap *et al.*, 2004), while we found normal levels of catecholamines in the adrenals and heart of adult *Th* knock-in mice (data not shown), which indicated central regulation for reduced body weight and hypotension. Normal catecholamine content in peripheral tissues was also reported for heterozygous *Th* knock-out mice that present a significant reduction of TH (Kobayashi *et al.*, 1995).

## Gradual loss of brain catecholamines in *Th* knock-in mice

Whole brain catecholamine and serotonin metabolites were measured in newborn (Day 1), juvenile (3 weeks) and adult
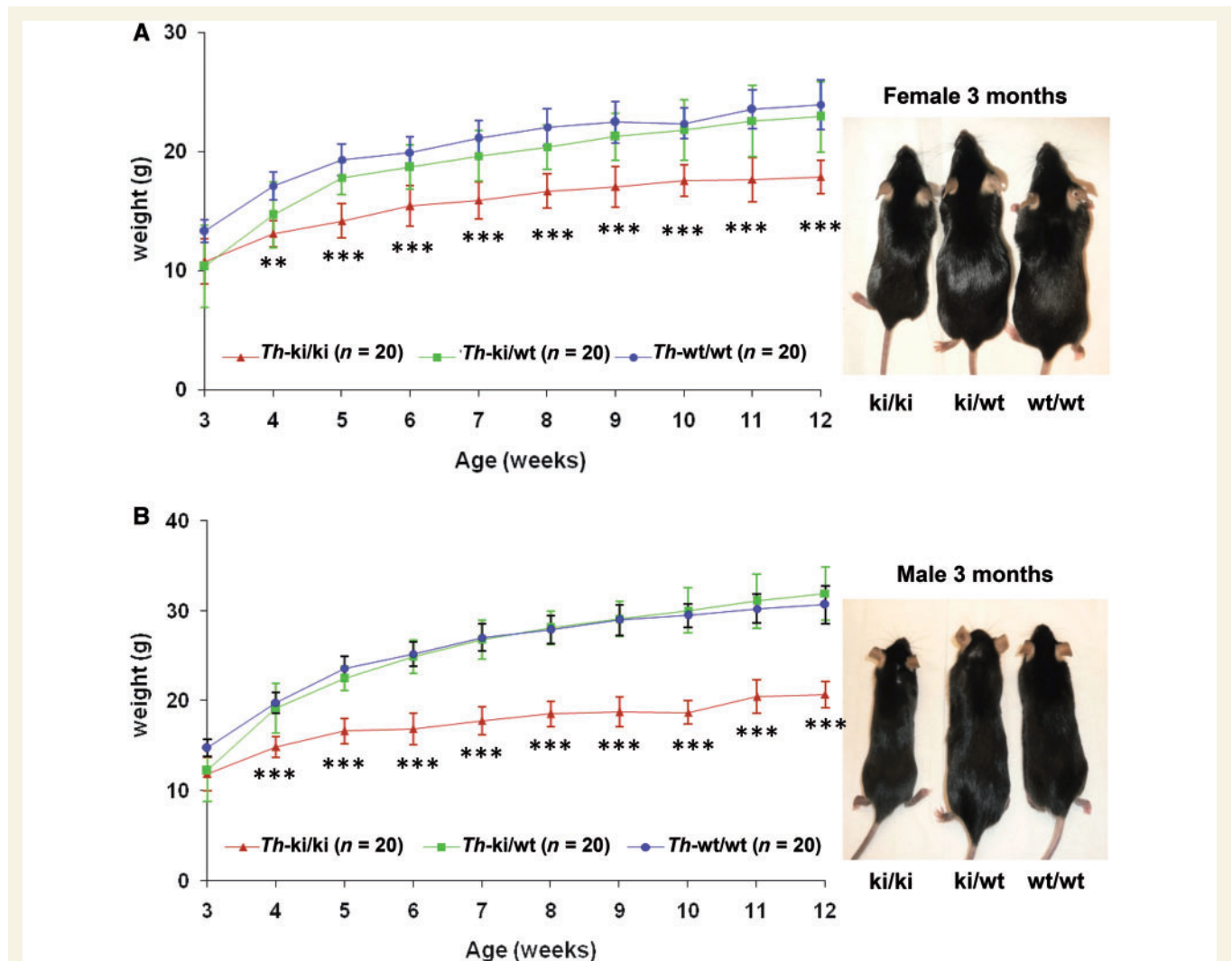


**Figure 1 Sex-specific differences in body weight between wild-type and *Th* knock-in mice.** (**A**) Female and (**B**) male mice fed *ad libitum* with standard chow. Growth retardation resulted in reduced body weight, for instance at the age of 12 weeks 25% reduction for females and 34% reduction for males. Significant differences between *Th* knock-in (ki) and wild-type (wt) combined with heterozygotes mice are indicated: **$P < 0.01$; ***$P < 0.001$ (Student's two-tailed *t*-test).

mice (12 weeks and 1 year). The values of brain dopamine and other catecholamines and their metabolites obtained for adult wild-type mice were in a similar range to those obtained in previous studies (Thöny *et al.*, 2008; Calvo *et al.*, 2010). HVA, the major biomarker in CSF for TH deficiency in patients, was low in *Th* knock-in mice at all ages, whereas L-DOPA, dopamine, norepinephrine and MHPG were initially normal, but fell continuously thereafter in mutant mice (Fig. 2A–D). This decrease appears specific for the catecholamines and their metabolites, as serotonin, which is typically not compromised in THD, remained unchanged both with respect to age and when compared with the values in wild-type mice, and only at an advanced age, when mutant mice exhibited a striking loss of catecholamines, was a reduction of the serotonin precursor 5-hydroxytryptophan (5-HTP) observed (Fig. 2D). Biopterin (and neopterin) content remained unchanged at all ages (Supplementary Fig. 4), as was the case for 5-HIAA, thus leading to a reduced HVA:5-HIAA ratio in *Th* knock-in mice compared to wild-type mice at all ages (Supplementary Table 2), similar to what is found in the CSF of THD patients (Willemsen *et al.*, 2010). Furthermore, we measured a consistent elevation of serum prolactin levels in adult mutant mice reflecting central dopamine deficiency (Supplementary Fig. 3D) that caused reduced fertility of *Th* knock-in females (not shown), although galactorrhoea was not observed.

## Early motor dysfunction and diurnal fluctuation of the motor deficits in *Th* knock-in mice

A moderate reduction of motor activity was observed in mutant mice during metabolic cage analyses (Supplementary Fig. 2C). To explore the nature of this motor dysfunction, we performed a series of behavioural tests assessing spontaneous catalepsy, motor coordination, amount and velocity of spontaneous locomotion, and gait characteristics at different ages. Motor function was tested in juvenile (3 weeks old), young adult (11 weeks old) and 1-year-old mutant male mice plus sex and age-matched wild-type controls (Fig. 3A–F). In the bar test, *Th* knock-in mice showed increased time of immobility compared to controls, indicating spontaneous catalepsy, a sign of rigidity and inability to initiate movements. In addition, when placed at the bar, *Th* knock-in mice of all ages, but particularly older adults, presented an abnormal body posture and muscle twitching, suggesting the presence of a dystonic component, while we did not observe clasping of the hindlimbs by the vertical tail suspension assay as a common test for a dystonic phenotype in mice (Sato *et al.*, 2008). *Th* knock-in male mice challenged in the rotarod test showed a significantly reduced latency to fall, indicating impaired motor coordination. In the open field test,
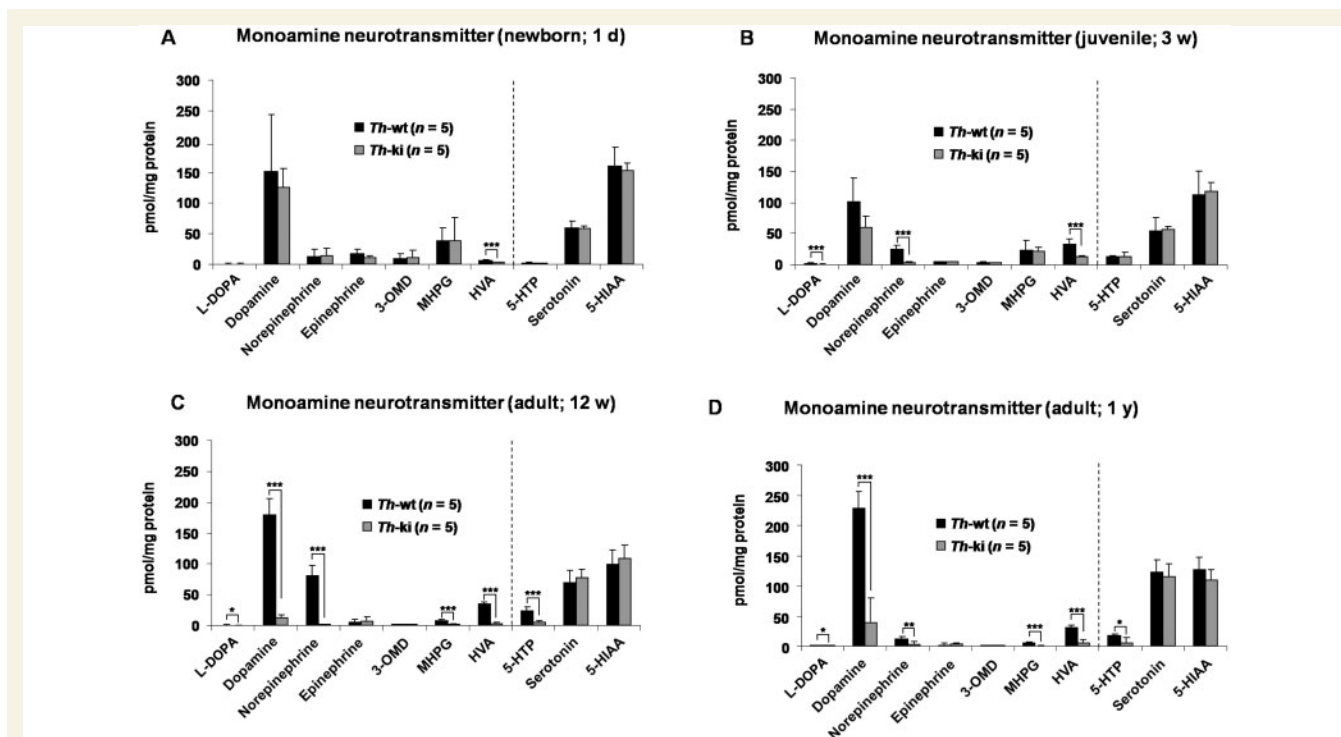


**Figure 2 Gradual loss of brain monoamine neurotransmitter metabolites in *Th* knock-in mice.** (**A**) Newborn mice, 1 day, (**B**) juvenile mice, 3 weeks, (**C**) adult mice, 12 weeks, and (**D**) adult mice, 1 year. Data for *Th* wild-type mice are shown in black and *Th* knock-in in grey. Monoamine neurotransmitter metabolites are depicted in pmol/mg of total brain protein. 3-OMD = 3-*O*-methlydopa; 5-HTP = 5-hydroxytryptophane. Significant difference from the corresponding wild-type value is indicated by asterisks: $*P < 0.05$; $**P < 0.01$; $***P < 0.001$ (Student's two-tailed *t*-test).
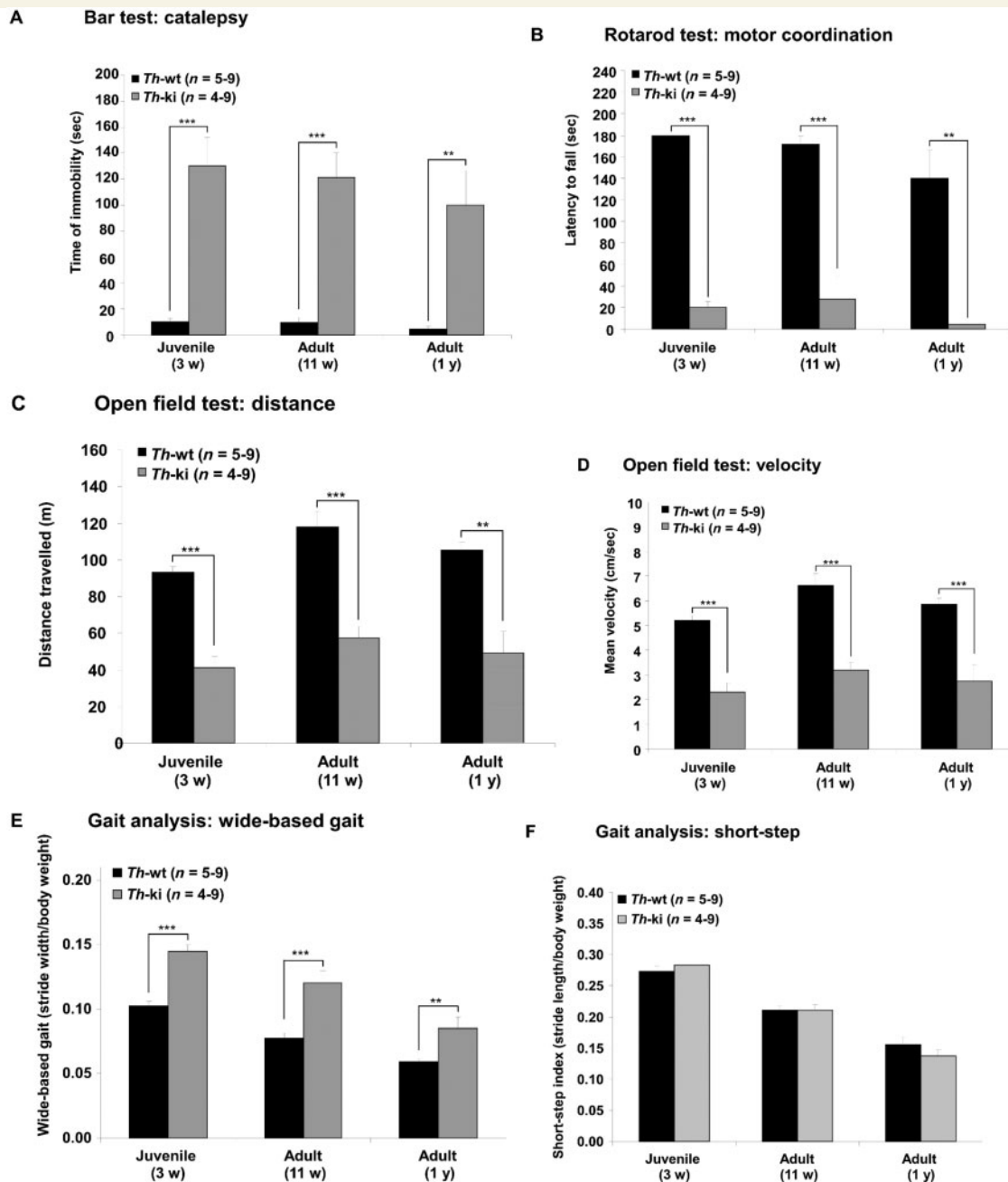
**Figure 3 Motor function tests of mutant (*Th* knock-in) and wild-type (*Th*-wild-type) male mice at different ages. (A)** Bar test for assessment of catalepsy. **(B)** Rotarod test for determination of motor coordination. **(C)** Total distance travelled in the open field test. **(D)** Mean velocity of locomotion in the open field test. **(E)** Gait analysis to test for stride width normalized to body weight. **(F)** Gait analysis to test for short-step disorder (stride length normalized to body weight). *Th* wild-type mice are shown in black and *Th* knock-in in grey. Significant difference from the corresponding wild-type value is indicated: **$P < 0.01$; ***$P < 0.001$ (Student's two-tailed $t$-test or ANOVA for fluctuation bar test).

*Th* knock-in mice showed significantly reduced levels of horizontal activity (amount and velocity of spontaneous locomotion), indicating a hypokinetic and bradykinetic phenotype. Next, we analysed the characteristics of gait (normalized to body weight to compensate for the size difference between genotypes). Mutant mice had an increased stride width per body weight index compared to normal controls, suggestive of a significant wide-based gait. This was confirmed by a generalized disorganization of the gait, including dragging marks, changes in direction and freezing (data not shown). In contrast, *Th* knock-in mice did not show abnormal stride length, as observed by an unchanged stride length per body weight index compared to controls. In summary, while the catecholamine deficiency increased with age (Fig. 2A–D), the severe motor dysfunction was present from the first measurements at 3 weeks onwards, and its severity appeared independent of age.
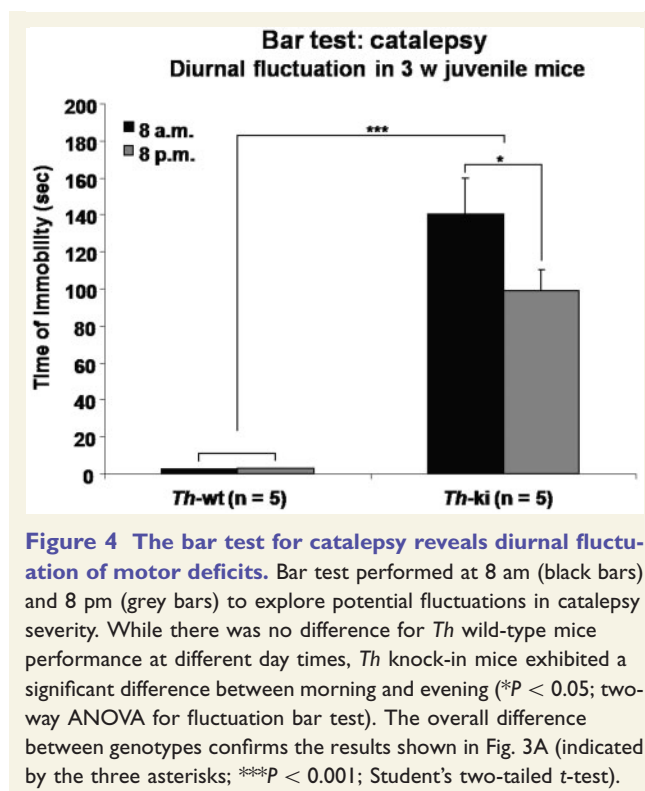
Marked diurnal fluctuation of motor behaviour is a hallmark in patients with THD (Willemsen *et al.*, 2010; Haugarvoll and Bindoff, 2011). To determine whether the motor performance in mutant mice varied throughout the day, we performed the bar test at 8 am and 8 pm in the same set of animals and found that *Th* knock-in mice performed significantly better after the resting period (at 8 pm, note the inverted circadian rhythms of mice compared to humans) than after the activity period (at 8 am), while wild-type controls presented a stable performance at both times (Willemsen *et al.*, 2010; Haugarvoll and Bindoff, 2011) (Fig. 4).

## Gradual reduction of TH protein and activity in brain of *Th* knock-in mice, with specific loss of TH in striatum

Gene expression of *Th*, *Tph*1 and *Tph*2 (mRNAs) in whole brain extracts of *Th* knock-in mice was similar to that in wild-type mice at different ages, and no particular heterogeneity was observed for transcript numbers in either mice. *Th* mRNA transcripts (but not *Tph*1 and *Tph*2 mRNAs) showed an increase of ~50% from newborn (1 day) to 3 weeks for both wild-type and *Th* knock-in mice (Supplementary Table 1). On the other hand, immunoquantification of TH protein content in whole brain extracts showed a remarkable 5-fold increase in TH relative to total protein from newborn to 3 weeks in normal mice, but no significant increase in TH protein was measured in this period for *Th* knock-in (Fig. 5A and B). For wild-type mice, TH content was maintained from 3 weeks up to 1 year, but *Th* knock-in revealed a gradual loss of TH protein relative to the normal (wild-type) content, reaching a value as low as ~3% of wild-type TH protein in 1-year-old animals (Fig. 5B, inset). The specific TH activity in brain extracts under standard conditions, measured by a sensitive radiochemical assay (Reinhard *et al.*, 1986), also followed a similar development as the protein content for the wild-type animals (the activity increased from $1.6 \pm 0.6$ to $5.3 \pm 1.0$ pmol L-DOPA/mg/min from Day 1 to 3 weeks, a value that was maintained up to 1 year). However, the activity in *Th* knock-in brain extracts was below the sensitivity threshold and could not be determined accurately by the radiochemical assay or other methods tested, including HPLC and fluorimetric detection of L-DOPA (Haavik and Flatmark, 1980).

Loss of TH was also observed by immunohistochemical staining for TH of the substantia nigra pars compacta and ventral tegmental area region and corpus striatum on coronal brain sections from perfused adult male *Th* knock-in and wild-type mice (6–7 months old). As seen in Fig. 5C we observed a similar expression pattern of TH in *Th* knock-in and control mice in the substantia nigra pars compacta/ventral tegmental area, with some less dense stained projections, whereas in the corpus striatum we observed an



**Figure 4 The bar test for catalepsy reveals diurnal fluctuation of motor deficits.** Bar test performed at 8 am (black bars) and 8 pm (grey bars) to explore potential fluctuations in catalepsy severity. While there was no difference for *Th* wild-type mice performance at different day times, *Th* knock-in mice exhibited a significant difference between morning and evening (*$P < 0.05$; two-way ANOVA for fluctuation bar test). The overall difference between genotypes confirms the results shown in Fig. 3A (indicated by the three asterisks; ***$P < 0.001$; Student's two-tailed *t*-test).

almost complete lack of immunoreactive processes. Furthermore, higher magnification photomicrographs depict a similar soma staining in the midbrain of mutants and controls whereas reduced staining of processes is again observed for the mutants (Fig. 5D). A semiquantitative TH + cell count performed in the substantia nigra pars compacta/ventral tegmental area of mutant and control brains indicated no decrease of immunoreactive TH cells in the midbrain of the mutants ($220.5 \pm 35.5$ and $232.5 \pm 35.5$ for *Th* knock-in and *Th* wild-type mice, respectively). Together with the lack of aberrant amyloid deposition in either midbrain or corpus striatum, as indicated by Congo red staining in these brain areas (Fig. 5E), the histological results strongly support lack of neurodegeneration in the midbrain of mutant animals. Rather, our results support the reduction in the amount of TH protein measured by immunoquantification and revealed a marked mislocalization of TH, consistent with a defective transport of mTH-R203H across the nigrostriatal projection (see below).

## The misfolding loss-of-function mutations hTH1-R202H and mTH-R203H are not stabilized by dopamine

To better understand the TH dysfunction in THD patients and in *Th* knock-in mice, we studied the molecular and kinetic effects of the mutation in the human (h) and mouse (m) TH enzymes, using purified, tetrameric,
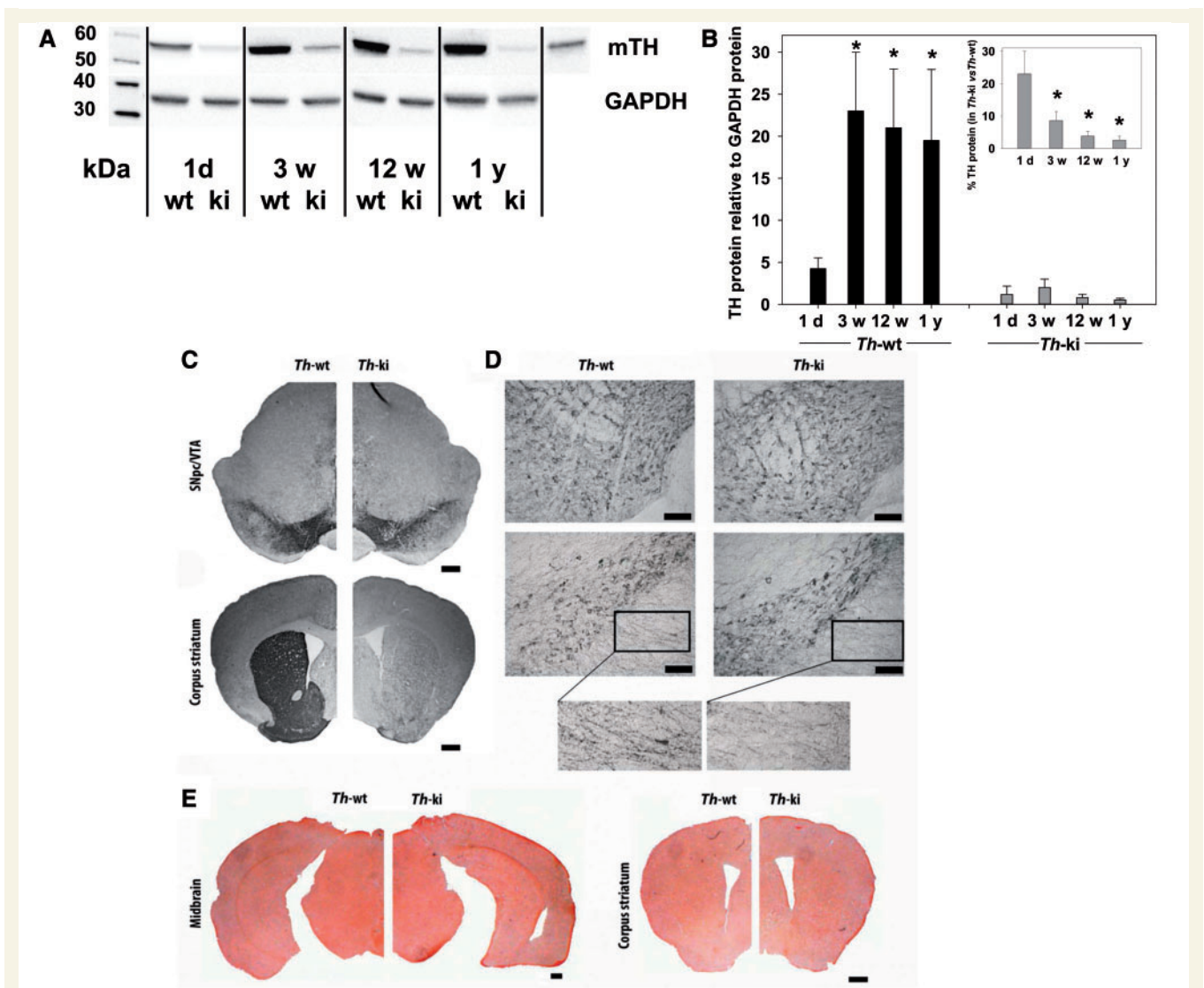
**Figure 5  TH protein content in brain from *Th*-wild-type and *Th* knock-in mice.** (**A**) Representative immunoblots of brain extracts of mice at the age of 1 day, 3 weeks, 12 weeks and 1 year; kDa, standard; mTH, purified mouse TH; wild-type (*Th*-wild-type) and ki (*Th* knock-in) mice. (**B**) TH protein content in brain extracts from *Th* wild-type (black bars) and *Th* knock-in mice (grey bars), as density of the 59 kDa TH band relative to the intensity of the GAPDH band. *Inset*: Percentage of TH protein content (grey bars) in brain extracts of *Th* knock-in versus *Th* wild-type mice. Significant difference between mice at different ages with mice at 1 day is indicated: *$P < 0.001$ (Student's two-tailed *t*-test). (**C–E**) Immunohistochemical and Congo red staining of TH in brain of *Th*-wild-type and *Th* knock-in mutant mice, at the age of 6–7 months. (**C**) Substantia nigra pars compacta (SNpc)/ventral tegmental area (VTA) of *Th* wild-type and *Th* knock-in mice present a similar degree of staining indicating lack of neurodegeneration in the mutant mice, while a striking lack of TH staining was observed in the corpus striatum in *Th* knock-in mice compared to wild-type control mice, indicating a largely reduced amount of TH protein in these neuronal processes. (**D**) Higher magnification view of midbrain TH + cell bodies at different levels (*top and middle panels*) and inset images depicting the higher density of processes staining in *Th* wild-type compared to *Th* knock-in brains (*bottom panel*). (**E**) Congo red staining in mutant and wild-type controls. The scale bars represent ∼0.5 mm (**C** and **E** *left*), ∼1.1 mm (**E**, *right*), and ∼100 μm (**D**).

recombinant hTH1-wt, mTH-wt, hTH1-R202H and mTH-R203H. First we analysed the substrate and cofactor-dependent activity of each enzyme (Supplementary Fig. 5A and B); the steady state activity constants are summarized in Table 1. Compared with hTH1-wt, mTH-wt showed reduced specific activity, but a similar $K_m(BH_4)$, slightly decreased $S_{0.5}(L\text{-Tyr})$ (higher substrate affinity for L-Tyr) and reduced substrate inhibition constant ($K_{si}$), denoting stronger substrate inhibition. The mutants

hTH1-R202H and mTH-R203H showed decreased $V_{max}$ and $K_m(BH_4)$ and slight increase of $S_{0.5}(L\text{-Tyr})$ compared with their corresponding wild-type counterparts, indicating a clear, but not severe kinetic defect. On the other hand, an evident destabilizing misfolding of the mutant enzymes was indicated by a 10-fold lower yield of purified tetrameric mutant enzymes expressed in *E. coli*, compared with the wild-type forms. Decreased protein stability of the hTH1-R202H mutant is also predicted by the FoldX algorithm

**Table 1** Steady-state kinetic parameters for recombinant purified human TH1 (hTH1) and mouse TH (mTH) wild-type (wt) forms, and the respective mutants hTH1-R202H and R203H

| Enzyme | BH$_4$ | | L-Tyr | | |
|---|---|---|---|---|---|
| | V$_{max}$ (nmol of L-DOPA/min×mg) | K$_m$ (BH$_4$) (µM) | V$_{max}$ (nmol of L-DOPA/min×mg) | S$_{0.5}$(L-Tyr) (µM) | K$_{si}$[a] (µM) |
| hTH1-wt | 400 ± 11 | 50 ± 6 | 782 ± 41 | 22 ± 1 | 54 ± 5 |
| mTH-wt | 252 ± 14[*] | 47 ± 10 | 583 ± 46[*] | 15 ± 1[*] | 28 ± 4[*] |
| hTH1-R202H | 162 ± 3[*] | 34 ± 3[*] | 344 ± 50[*] | 28 ± 3 | 60 ± 9 |
| mTH-R203H | 132 ± 3[**] | 21 ± 2[**] | 280 ± 40[**] | 23 ± 5 | 49 ± 6[**] |

For BH$_4$ concentration dependency, data were fit to the Michaelis-Menten model and for L-Tyr concentration dependency to the substrate inhibition model.
[a]K$_{si}$, substrate inhibition constant.
[*] $P < 0.05$ with respect to corresponding values for hTH1-wt.
[**] $P < 0.05$ with respect to corresponding values for mTH-wt.
See also Supplementary Fig. 5. Results are means ± SD for three different experiments.

(Schymkowitz *et al.*, 2005), which estimated a destabilization energy of 9.96 kcal/mol ($\Delta\Delta G$) based on the tetrameric structure of hTH (PDB 2XSN), including the catalytic and tetramerization domains. To corroborate that the mutation caused the destabilization, we performed differential scanning fluorimetry (DSF) analyses. This method was chosen due to the small amounts of protein required, as protein was limited for the mutants. The mutant enzymes showed reduced stability compared with the respective wild-type forms [2–3°C decreased midpoint denaturation ($T_m$)-values; Fig. 6A]. Although significant, the decreased thermodynamic stability caused by the mutation could not, however, fully explain the relative decay of TH protein in the *Th* knock-in compared to the wild-type mouse (Fig. 5). Additional defects in regulatory stabilization of the mutant mTH-R203H enzyme might explain this relative loss of TH protein in the mutant mouse. Stabilization of TH by dopamine and other catecholamines is an important regulatory mechanism, which leads to competitive inhibition of TH activity versus the BH$_4$ cofactor, and provides a natural chaperone effect that prevents degradation of the enzyme (Okuno and Fujisawa, 1991; Sumi-Ichinose *et al.*, 2001; Thöny *et al.*, 2008). *In vitro*, this stabilization is manifested by an increase in the $T_m$-values and a decrease in its susceptibility to proteolysis (Martinez *et al.*, 1996; McCulloch and Fitzpatrick, 1999). As expected, hTH1-wt and mTH-wt were stabilized by dopamine binding, increasing their $T_m$-values up to 3°C (Fig. 6A and B), but the mutants were not stabilized by dopamine (Fig. 6C and D). In addition, dopamine protected the wild-type enzymes, but not the mutants, from limited tryptic proteolysis (shown for hTH1 in Fig. 6E–K).

## Non-responsiveness of *Th* knock-in mice to L-DOPA treatment

We determined the effect of chronic and acute L-DOPA treatment on the motor outcome of juvenile or young adult *Th* knock-in mice and controls. In the chronic tests, catalepsy and motor coordination were investigated after daily L-DOPA (plus carbidopa) or mock treatment from birth to 3 weeks of age using a high dose according to recommendations for THD in humans (i.e. 10 mg/kg/day of L-DOPA) (Willemsen *et al.*, 2010). No significant differences were found either in the bar test or rotarod performance in *Th* knock-in mice given L-DOPA or vehicle (Supplementary Fig. 6A and B). Similar negative results were obtained from treating adult *Th* knock-in mice over a period of 12 days (not shown). Nevertheless, monoamine neurotransmitter analysis in brain extracts of sacrificed mice showed significant metabolite improvement following L-DOPA treatment (Fig. 7A), although TH protein was not increased (Fig. 7B). Similarly, in an acute test for motor coordination (rotarod) and catalepsy or rigidity (bar test) upon a single dose of L-DOPA (10 mg per kg body weight plus carbidopa), *Th* knock-in mice did not show any differences in performance before and 20–45 min after administration (Supplementary Fig. 6C and D), corroborating non-responsiveness of *Th* knock-in mice to L-DOPA treatment.

## Discussion

The *Th* knock-in mouse was generated to provide an experimental *in vivo* model to investigate TH and catecholamine deficiency both in terms of disease pathogenesis and the effect of mutations on enzyme function and regulation *in vivo*. In the longer term, this model appears valuable to test treatments aimed at improving diseases related to loss of dopamine. The model is clinically robust. The *Th* knock-in mouse appears normal at birth, but thereafter exhibits moderate failure to thrive, motor abnormalities including abnormal body posture and twitching, i.e. dystonia-like features, reduced coordination, hypokinesia, ataxia and catalepsy or rigidity-akinesia. There is also clear diurnal variation of the motor defects and lowered blood pressure, as found in THD patients homozygous for p.Arg233His (Willemsen *et al.*, 2010). The biochemical and other abnormalities in the *Th* knock-in mice include an early and persistent decrease in brain dopamine and noradrenaline to critically low levels, associated with low brain TH, which together with a
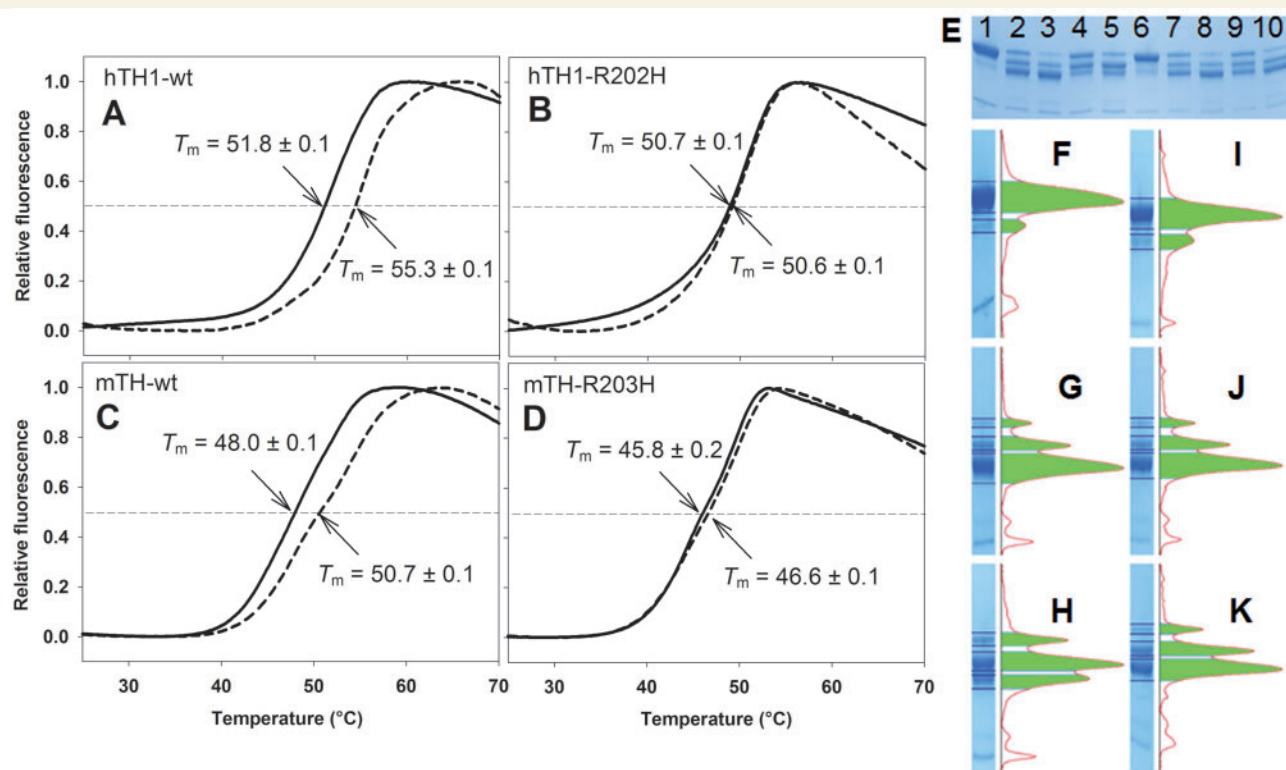
**Figure 6  The stability of recombinant purified human TH1 (hTH1) and mouse TH (mTH) and the respective mutants R202H and R203H, and effect of dopamine. (A–D)** Differential scanning fluorimetry profiles (fluorescence at 610 nm versus temperature) for hTH1-wt (**A**), mTH-wt (**B**), hTH1-R202H (**C**) and mTH-R203 (**D**), analysed at a concentration of 0.9 μM subunit without (solid black line) and with (dotted line) equimolar amount (0.9 μM) of dopamine. The midpoint denaturation ($T_m$)-values, determined as maximal temperature in first-derivatives, are shown in the corresponding plots. (**E**) SDS-PAGE showing the limited tryptic digestion of hTH1-wt (lanes 1–5) and hTH1-R202H (lanes 6–10) in the absence (2, 3, 7, 8) and the presence (4,5,9,10) of 50 μM dopamine; 1 and 6 are the respective controls in the absence of trypsin. Conditions: 2.5 μM subunit hTH1 or hTH1-R202H were incubated with trypsin for 30 s (2, 4, 7, 9) or 60 s (3, 5, 8, 10) at 25°C, at a TH:trypsin ratio of 200:1. The gels were stained with Coomassie Brilliant Blue and the raw area of the bands was measured using the Image Lab 3.0.1 software, and represented for lanes 1, 3, 5, 6, 8 and 10 in **F, G, H, I, J** and **K**, respectively. At the selected conditions, hTH1-wt (apparent molecular weight of 59 kDa), was trypsinized into two truncated forms of 57 and 54 kDa, both lacking the N-terminal peptide MPTPDATTPQAKGFR (analyses by LC–MS/MS spectroscopy; data not shown).

reduced body weight and hyperprolactinaemia are characteristics of THD. *Th* knock-in mice were notably homogeneous with respect to all parameters determined in this work, including motor dysfunction, biochemical phenotype and unresponsiveness to L-DOPA, which probably reflects the genetic background homogeneity of these inbred strains. Patients homozygous for p.Arg233His actually show higher phenotypic variability (Willemsen *et al.*, 2010), which might point to THD as a complex trait autosomal recessive disorder where the phenotype might be modulated at different steps of the catecholaminergic systems, reflecting a higher complexity in human than mice.

Previous mice models have not mirrored THD to the same degree as the here presented *Th* knock-in mouse. Both the *Th*$^{-/-}$ and the dopamine β-hydroxylase-deficient *Dbh*$^{-/-}$ knock-out mice have a high pre- and perinatal mortality due to cardiovascular failure associated with the lack of norepinephrine, and confirm the importance of catecholamines for foetal development (Kobayashi *et al.*, 1995; Thomas *et al.*, 1995; Zhou *et al.*, 1995). TH function

and norepinephrine synthesis could be rescued in noradrenergic neurons of transgenic *Th*$^{-/-}$ mice. These dopamine-deficient mice survive for a short period without treatment (Willemsen *et al.*, 2010; Garcia-Cazorla and Duarte, 2014), but have normal norepinephrine levels and are thus imperfect models for THD. The aromatic amino acid decarboxylase knock-out mouse is catecholamine-deficient and shows a 50% survival, but shows in addition seriously reduced serotonin levels (Lee *et al.*, 2013) and is also not a model to investigate the pathogenic mechanisms of specific TH deficiency.

Newborn *Th* knock-in mice show normal values of catecholamines and other metabolites, except for a reduction in HVA. By 3 weeks of age, however, we observed a drop in brain norepinephrine that, despite its crucial role in mouse foetal development (Thomas *et al.*, 1995), did not affect pup survival. Initially, the reduction in norepinephrine was not accompanied by any significant decrease in dopamine, pointing to compensatory mechanisms that maintain dopamine levels e.g. by downregulation of its
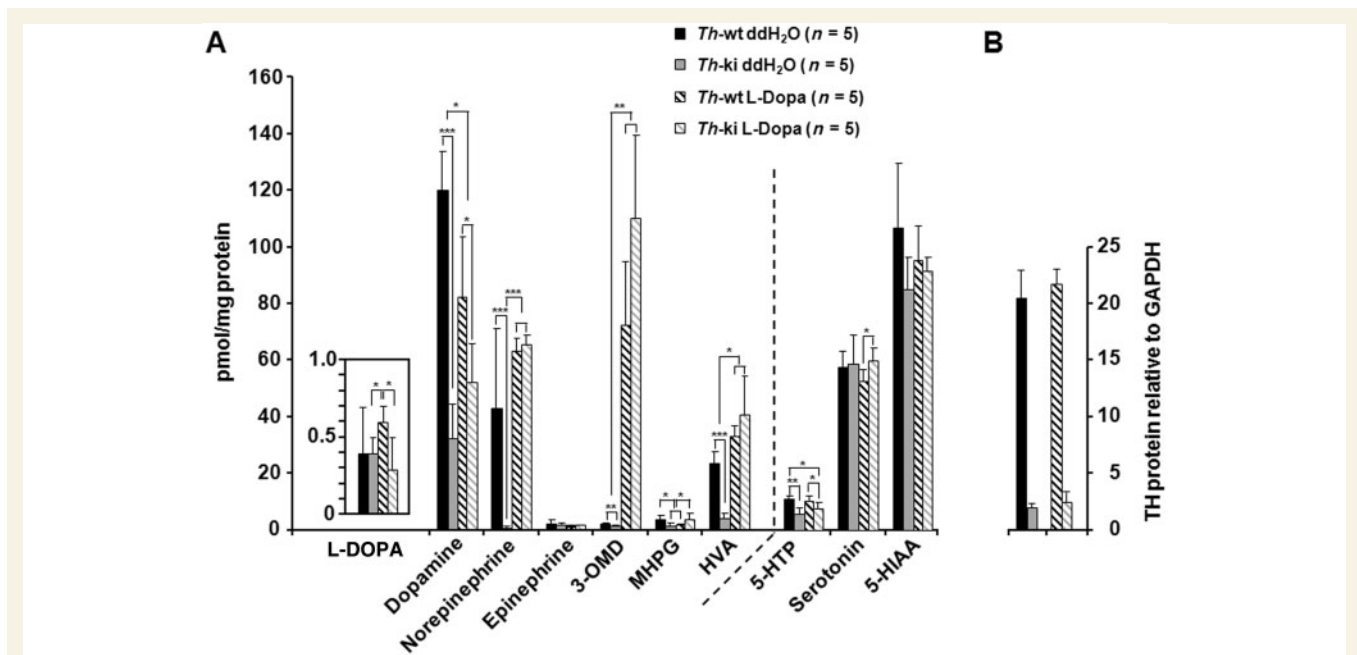
**Figure 7** Outcome of L-DOPA treatment of *Th* knock-in mice on brain monoamine neurotransmitter metabolites and TH protein. Mutant *Th* knock-in (ki) and *Th* wild-type (wt) mice were treated from Day 1 after birth onwards for a period of 3 weeks with L-DOPA (10 mg/kg/day) plus carbidopa (2.5 mg/kg/day) or vehicle (ddH$_2$0 control); *inset*, L-DOPA in pmol/mg protein. (**A**) Brain monoamine neurotransmitter metabolites. (**B**) TH protein relative to GAPDH is shown for *Th* wild-type and *Th* knock-in mice with or without L-DOPA/carbidopa treatment. In both **A** and **B**, significant difference from the corresponding wild-type value is indicated: *$P < 0.05$; **$P < 0.01$; ***$P < 0.001$ (Student's two-tailed *t*-test).

degradation (Tunbridge *et al.*, 2006). Concomitant to their defective brain noradrenaline content, *Th* knock-in mice fail to accomplish the 5-fold increase in TH protein observed for the *Th* wild-type mice from newborn to 3 weeks of age (Fig. 5B), despite the presence of normal (similar to wild-type) levels of *Th*-mRNA (Supplementary Table 1). A similar substantial increase in TH in the same postnatal period has been reported, and this increase appears critical for the correct development of the dopaminergic system and the psychomotor function (Homma *et al.*, 2011). This finding is supported by our results showing early and persistent motor dysfunction in the *Th* knock-in mice. The postnatal increase in TH protein in normal mice is not only driven by upregulated transcription (Supplementary Table 1) but through stabilization of the TH protein, where both the level of BH$_4$ and catecholamines themselves have been shown to be implicated in the stabilization (Homma *et al.*, 2011, 2013). BH$_4$ levels are similar in *Th* wild-type and knock-in mice, and the $K_m$(BH$_4$) for the mutant enzymes indicates a relative high affinity for the cofactor (Table 1). Catecholamine binding and feedback inhibition of TH occur in competition with BH$_4$ (Nagatsu, 1995; Daubner *et al.*, 2011), and thus the enzyme kinetics data are in accord with a mutation-associated structural change in TH that leads to opposite effects for BH$_4$ and dopamine, and to defective stabilization by dopamine (or norepinephrine; data not shown). Despite some recent insights on residues important for catecholamine binding at the catalytic domain (Briggs *et al.*,

2014), a structural explanation for the defective stabilization by dopamine in the mutants must await the determination of high resolution structures of full-length TH, including the regulatory domain, where the determinants for high affinity binding are located (McCulloch and Fitzpatrick, 1999; Nakashima *et al.*, 1999). The hTH1-R202H and mTH-R203 mutants show both kinetic (Table 1) and stability defects (Fig. 6), but the lack of dopamine stabilization of mutant TH emerges as a deleterious regulatory deficiency that explains the lack of accumulation of TH protein in the critical postnatal period in the *Th* knock-in mice (Fig. 5A and B). Defective stabilization by catecholamines may also support the specific deficit of TH expression in the striatum (Fig. 5C and D) as proper transport of TH to this brain area also requires the stabilization of the enzyme (Homma *et al.*, 2013). Mutation-associated defective trafficking and aberrant localization of protein cargos is a recurrent pathological mechanism in neurological and neurodegenerative disorders (Hung and Link, 2011; Encalada and Goldstein, 2014). Little is known about mechanisms of transport of TH and dopamine in the dopaminergic nigrostriatal pathway projecting from the substantia nigra pars compacta to the caudate-putamen (striatum), although it is accepted that at least in adrenergic neuronal systems, TH is fast transported along the axon in an anterograde fashion to the terminals (Brimijoin and Wiermaa, 1977). Accordingly, impaired axonal transport of TH in dopaminergic projections has recently been shown to be associated with parkinsonism and drastic

reduction of TH and dopamine levels in striatal synapses (Ittner *et al.*, 2008). It is thus very probable that the observed motor dysfunction in the *Th* knock-in mice is caused by defective TH protein transport leading to scarce TH and dopamine in synaptic terminals to activate dopamine receptors in the caudate-putamen.

Lack of or poor responsiveness to L-DOPA is manifested by a large number of patients with THD type B, particularly those with the hTH1-R202H mutation (Grattan-Smith *et al.*, 2002; Willemsen *et al.*, 2010). One interesting finding of the present study is that the motor dysfunction of the *Th* knock-in mice is not improved by standard L-DOPA supplementation even when treated from the first day of life. Other mouse models with dopamine deficiency show a partial recovery with dopamine treatment, especially in features such as feeding problems. Motor improvement is, however, often incomplete (Zhou and Palmiter, 1995), reflecting perhaps the developmental deficiencies in the foetal and perinatal periods (Zhou and Palmiter, 1995; Homma *et al.*, 2011). Possible neurodevelopment disorders associated with defective stabilization by catecholamines and consequent mislocalization of TH cannot be ruled out as the reason for the lack of DOPA-responsiveness of the motor dysfunction in the *Th* knock-in mice, despite the apparent correction of L-DOPA levels and increase of dopamine in brain extracts observed after treatment (Fig. 7). Developing novel non-L-DOPA-based therapeutic strategies for THD type B may thus be an attractive approach, especially for patients with the specific h*TH*-R233H mutation. In this respect, emerging therapies based on protein stabilization, e.g. pharmacological chaperones, appear promising, as we have previously shown in *in vitro* experiments that the variant hTH1-R202H can be stabilized by compounds with chaperone potential (Calvo *et al.*, 2010; Hole *et al.*, 2015). Furthermore, the diurnal fluctuation of motor deficits is definitively an important hallmark of our *Th* knock-in mutant mouse and may also be exploited in the search for novel treatment strategies based on the restorative potential of either circadian regulation of TH activity and/or restorative properties of sleep.

Finally, the growth retardation measured in the *Th* knock-in mutant mouse in combination with normal food intake, normoglycaemia and apparent reduced energy expenditure in the metabolic cage deserves explanation. Surviving mice with selective dopamine deficiency in dopaminergic neurons, but not in noradrenergic neurons, exhibit abnormal feeding behaviour including swallowing difficulties (aphagy) (Zhou and Palmiter, 1995; Szczypka *et al.*, 1999), symptoms we did not observe in the *Th* knock-in mice. On the other hand, growth retardation in combination with normal food intake has also previously been found in total and neuron-specific dopamine-receptor knock-out mice, which shows reduced dopamine signalling (Baik *et al.*, 1995; Noain *et al.*, 2013). Like these other surviving TH-deficient mice with reduced noradrenergic

activity, the *Th* knock-in mice presented here showed lowered resting metabolic rate with respect to wild-type mice. Furthermore, it has become increasingly clear that isolated dopaminergic abnormalities and parkinsonian syndromes involve abnormal or increased energy expenditure during walking and motor tasks which may explain the reduction in growth of mutant mice despite comparable food intake with wild-type mice (Molero-Luis *et al.*, 2013; Amano *et al.*, 2014).

In conclusion, there is a large spectrum of phenotypes in patients with THD, resulting from diverse deficiencies in absolute and relative dopamine and norepinephrine levels with different impact on systemic and motor function (Willemsen *et al.*, 2010). This variability would depend on the catalytic, conformational and regulatory defects of the particular TH mutation. In agreement with severely affected patients homozygous for the mutation p.R233H, *Th* knock-in mice studied in this work present severe motor deficiencies from a juvenile age onwards, and these abnormalities are apparently not corrected by classical replacement treatment with L-DOPA. The mutant hTH1-R202H and mTH-R203H proteins are not stabilized by dopamine, leading to intracellular instability, gradual loss of TH activity and altered nigro-striatal distribution, aiding to interpret the biochemical and locomotor phenotype of *Th* knock-in. In addition, to contribute to the understanding of the biochemical pathogenesis of catecholamine deficiency, this mouse model offers a useful platform for designing and evaluating new routes to disease therapies not only for THD, but also other genetic and idiopathic dopaminergic deficiencies.

# Acknowledgements

# Funding

# Supplementary material

Supplementary material is available at *Brain* online.

# References

Aitkenhead H, Heales SJ. Establishment of paediatric age-related reference intervals for serum prolactin to aid in the diagnosis of neurometabolic conditions affecting dopamine metabolism. Ann Clin Biochem 2013; 50(Pt 2): 156–8.

Amano S, Kegelmeyer D, Hong SL. Rethinking energy in parkinsonian motor symptoms: a potential role for neural metabolic deficits. Front Syst Neurosci 2014; 8: 242.

Avale ME, Falzone TL, Gelman DM, Low MJ, Grandy DK, Rubinstein M. The dopamine D4 receptor is essential for hyperactivity and impaired behavioral inhibition in a mouse model of attention deficit/hyperactivity disorder. Mol Psychiatry 2004; 9: 718–26.

Baik JH, Picetti R, Saiardi A, Thiriet G, Dierich A, Depaulis A, et al. Parkinsonian-like locomotor impairment in mice lacking dopamine D2 receptors. Nature 1995; 377: 424–8.

Bello EP, Mateo Y, Gelman DM, Noain D, Shin JH, Low MJ, et al. Cocaine supersensitivity and enhanced motivation for reward in mice lacking dopamine D2 autoreceptors. Nat Neurosci 2011; 14: 1033–8.

Ben-Jonathan N. Dopamine: a prolactin-inhibiting hormone. Endocr Rev 1985; 6: 564–89.

Bjorklund A, Dunnett SB. Dopamine neuron systems in the brain: an update. Trends Neurosci 2007; 30: 194–202.

Blau N, Thony B, Renneberg A, Penzien JM, Hyland K, Hoffmann GF. Variant of dihydropteridine reductase deficiency without hyperphenylalaninaemia: effect of oral phenylalanine loading. J Inherit Metab Dis 1999; 22: 216–20.

Bohnen NI, Jahn K. Imaging: what can it tell us about parkinsonian gait? Mov Disord 2013; 28: 1492–500.

Bornstein SR, Tian H, Haidan A, Bottner A, Hiroi N, Eisenhofer G, et al. Deletion of tyrosine hydroxylase gene reveals functional interdependence of adrenocortical and chromaffin cell system *in vivo*. Proc Natl Acad Sci USA 2000; 97: 14742–7.

Briggs GD, Bulley J, Dickson PW. Catalytic domain surface residues mediating catecholamine inhibition in tyrosine hydroxylase. J Biochem 2014; 155: 183–93.

Brimijoin S, Wiermaa MJ. Rapid axonal transport of tyrosine hydroxylase in rabbit sciatic nerves. Brain Res 1977; 121: 77–96.

Calvo AC, Scherer T, Pey AL, Ying M, Winge I, McKinney J, et al. Effect of pharmacological chaperones on brain tyrosine hydroxylase and tryptophan hydroxylase 2. J Neurochem 2010; 114: 853–63.

Catafau AM, Bullich S. Amyloid PET imaging: applications beyond Alzheimer's disease. Clin Transl Imaging 2015; 3: 39–55.

Daubner SC, Le T, Wang S. Tyrosine hydroxylase and regulation of dopamine synthesis. Arch Biochem Biophys 2011; 508: 1–12.

de Medinaceli L, Freed WJ, Wyatt RJ. An index of the functional condition of rat sciatic nerve based on measurements made from walking tracks. Exp Neurol 1982; 77: 634–43.

Delafontaine P, Song YH, Li Y. Expression, regulation, and function of IGF-1, IGF-1R, and IGF-1 binding proteins in blood vessels. Arterioscler Thromb Vasc Biol 2004; 24: 435–44.

Eisenhofer G, Kopin IJ, Goldstein DS. Catecholamine metabolism: a contemporary view with implications for physiology and medicine. Pharmacol Rev 2004; 56: 331–49.

Elzaouk L, Leimbacher W, Turri M, Ledermann B, Burki K, Blau N, et al. Dwarfism and low insulin-like growth factor-1 due to dopamine depletion in Pts-/- mice rescued by feeding neurotransmitter precursors and H4-biopterin. J Biol Chem 2003; 278: 28303–11.

Encalada SE, Goldstein LS. Biophysical challenges to axonal transport: motor-cargo deficiencies and neurodegeneration. Annu Rev Biophys 2014; 43: 141–69.

Fossbakk A, Kleppe R, Knappskog PM, Martinez A, Haavik J. Functional studies of tyrosine hydroxylase missense variants reveal distinct patterns of molecular defects in dopa-responsive dystonia. Hum Mutat 2014; 35: 880–90.

Garcia-Cazorla A, Duarte ST. Parkinsonism and inborn errors of metabolism. J Inherit Metab Dis 2014; 37: 627–42.

Gelman DM, Noain D, Avale ME, Otero V, Low MJ, Rubinstein M. Transgenic mice engineered to target Cre/loxP-mediated DNA recombination into catecholaminergic neurons. Genesis 2003; 36: 196–202.

Grattan-Smith PJ, Wevers RA, Steenbergen-Spanjers GC, Fung VS, Earl J, Wilcken B. Tyrosine hydroxylase deficiency: clinical manifestations of catecholamine insufficiency in infancy. Mov Disord 2002; 17: 354–9.

Haavik J, Blau N, Thony B. Mutations in human monoamine-related neurotransmitter pathway genes. Hum Mutat 2008; 29: 891–902.

Haavik J, Flatmark T. Rapid and sensitive assay of tyrosine 3-monooxygenase activity by high-performance liquid chromatography using the native fluorescence of DOPA. J Chromatogr 1980; 198: 511–5.

Haugarvoll K, Bindoff LA. A novel compound heterozygous tyrosine hydroxylase mutation (p.R441P) with complex phenotype. J Parkinsons Dis 2011; 1: 119–22.

Hole M, Underhaug J, Diez H, Ying M, Røhr ÅK, Jorge-Finnigan A, et al. Discovery of compounds that protect tyrosine hydroxylase activity through different mechanisms. Biochim Biophys Acta 2015; 1854: 1078–89.

Homma D, Katoh S, Tokuoka H, Ichinose H. The role of tetrahydrobiopterin and catecholamines in the developmental regulation of tyrosine hydroxylase level in the brain. J Neurochem 2013; 126: 70–81.

Homma D, Sumi-Ichinose C, Tokuoka H, Ikemoto K, Nomura T, Kondo K, et al. Partial biopterin deficiency disturbs postnatal development of the dopaminergic system in the brain. J Biol Chem 2011; 286: 1445–52.

Hung MC, Link W. Protein localization in disease and therapy. J Cell Sci 2011; 124(Pt 20): 3381–92.

Ittner LM, Fath T, Ke YD, Bi M, van Eersel J, Li KM, et al. Parkinsonism and impaired axonal transport in a mouse model of frontotemporal dementia. Proc Natl Acad USA 2008; 105: 15997–6002.

Kobayashi K, Morita S, Sawada H, Mizuguchi T, Yamada K, Nagatsu I, et al. Targeted disruption of the tyrosine hydroxylase locus results in severe catecholamine depletion and perinatal lethality in mice. J Biol Chem 1995; 270: 27235–43.

Krege JH, Hodgin JB, Hagaman JR, Smithies O. A noninvasive computerized tail-cuff system for measuring blood pressure in mice. Hypertension 1995; 25: 1111–5.

Kumer SC, Vrana KE. Intricate regulation of tyrosine hydroxylase activity and gene expression. J Neurochem 1996; 67: 443–62.

Kunkel-Bagden E, Dai HN, Bregman BS. Methods to assess the development and recovery of locomotor function after spinal cord injury in rats. Exp Neurol 1993; 119: 153–64.

Kurian MA, Gissen P, Smith M, Heales S, Jr, Clayton PT. The monoamine neurotransmitter disorders: an expanding range of neurological syndromes. Lancet Neurol 2011; 10: 721–33.

Lee NC, Shieh YD, Chien YH, Tzen KY, Yu IS, Chen PW, et al. Regulation of the dopaminergic system in a murine model of aromatic L-amino acid decarboxylase deficiency. Neurobiol Dis 2013; 52: 177–90.

Livak KJ, Schmittgen TD. Analysis of relative gene expression data using real-time quantitative PCR and the 2(-Delta Delta C(T)) Method. Methods 2001; 25: 402–8.

Martinez A, Haavik J, Flatmark T, Arrondo JL, Muga A. Conformational properties and stability of tyrosine hydroxylase studied by infrared spectroscopy. Effect of iron/catecholamine binding and phosphorylation. J Biol Chem 1996; 271: 19737–42.

McCulloch RI, Fitzpatrick PF. Limited proteolysis of tyrosine hydroxylase identifies residues 33-50 as conformationally sensitive to phosphorylation state and dopamine binding. Arch Biochem Biophys 1999; 367: 143–5.

Molero-Luis M, Serrano M, Ormazabal A, Perez-Duenas B, Garcia-Cazorla A, Pons R, et al. Homovanillic acid in cerebrospinal fluid of 1388 children with neurological disorders. Dev Med Child Neurol 2013; 55: 559–66.

Nagatsu T. Tyrosine hydroxylase: human isoforms, structure and regulation in physiology and pathology. Essays Biochem 1995; 30: 15–35.

Nagatsu T, Levitt M, Udenfriend S. Tyrosine Hydroxylase. The Initial Step In Norepinephrine Biosynthesis. J Biol Chem 1964; 239: 2910–7.

Nakashima A, Mori K, Suzuki T, Kurita H, Otani M, Nagatsu T, et al. Dopamine inhibition of human tyrosine hydroxylase type 1 is controlled by the specific portion in the N-terminus of the enzyme. J Neurochem 1999; 72: 2145–53.

Noain D, Perez-Millan MI, Bello EP, Luque GM, Casas Cordero R, Gelman DM, et al. Central dopamine D2 receptors regulate growth-hormone-dependent body growth and pheromone signaling to conspecific males. J Neurosci 2013; 33: 5834–42.

Obeso JA, Rodriguez-Oroz MC, Goetz CG, Marin C, Kordower JH, Rodriguez M, et al. Missing pieces in the Parkinson's disease puzzle. Nat Med 2010; 16: 653–61.

Okuno S, Fujisawa H. Conversion of tyrosine hydroxylase to stable and inactive form by the end products. J Neurochem 1991; 57: 53–60.

Reed MC, Lieb A, Nijhout HF. The biological significance of substrate inhibition: a mechanism with diverse functions. Bioessays 2010; 32: 422–9.

Reinhard JF, Jr, Smith GK, Nichol CA. A rapid and sensitive assay for tyrosine-3-monooxygenase based upon the release of 3H2O and adsorption of [3H]-tyrosine by charcoal. Life Sci 1986; 39: 2185–9.

Roberts KM, Fitzpatrick PF. Mechanisms of tryptophan and tyrosine hydroxylase. IUBMB Life 2013; 65: 350–7.

Sato K, Sumi-Ichinose C, Kaji R, Ikemoto K, Nomura T, Nagatsu I, et al. Differential involvement of striosome and matrix dopamine systems in a transgenic model of dopa-responsive dystonia. Proc Natl Acad Sci USA 2008; 105: 12551–6.

Schymkowitz J, Borg J, Stricher F, Nys R, Rousseau F, Serrano L. The FoldX web server: an online force field. Nucleic Acids Res 2005; 33:W382–8.

Sumi-Ichinose C, Urano F, Kuroda R, Ohye T, Kojima M, Tazawa M, et al. Catecholamines and serotonin are differently regulated by tetrahydrobiopterin. A study from 6-pyruvoyltetrahydropterin synthase knockout mice. J Biol Chem 2001; 276: 41150–60.

Suresh Babu R, Sunandhini RL, Sridevi D, Periasamy P, Namasivayam A. Locomotor behavior of bonnet monkeys after spinal contusion injury: footprint study. Synapse 2012; 66: 509–21.

Swoap SJ, Weinshenker D, Palmiter RD, Garber G. Dbh(-/-) mice are hypotensive, have altered circadian rhythms, and have abnormal responses to dieting and stress. Am J Physiol Regul Integr Comp Physiol 2004; 286:R108–13.

Szczypka MS, Rainey MA, Kim DS, Alaynick WA, Marck BT, Matsumoto AM, et al. Feeding behavior in dopamine-deficient mice. Proc Natl Acad Sci USA 1999; 96: 12138–43.

Tank AW, Xu L, Chen X, Radcliffe P, Sterling CR. Post-transcriptional regulation of tyrosine hydroxylase expression in adrenal medulla and brain. Ann N Y Acad Sci 2008; 1148: 238–48.

Thomas SA, Matsumoto AM, Palmiter RD. Noradrenaline is essential for mouse fetal development. Nature 1995; 374: 643–6.

Thöny B, Calvo AC, Scherer T, Svebak RM, Haavik J, Blau N, et al. Tetrahydrobiopterin shows chaperone activity for tyrosine hydroxylase. J Neurochem 2008; 106: 672–81.

Tunbridge EM, Harrison PJ, Weinberger DR. Catechol-o-methyltransferase, cognition, and psychosis: Val158Met and beyond. Biol Psychiatry 2006; 60: 141–51.

Willemsen MA, Verbeek MM, Kamsteeg EJ, de Rijk-van Andel JF, Aeby A, Blau N, et al. Tyrosine hydroxylase deficiency: a treatable disorder of brain catecholamine biosynthesis. Brain 2010; 133(Pt 6): 1810–22.

Wueest S, Mueller R, Bluher M, Item F, Chin AS, Wiedemann MS, et al. Fas (CD95) expression in myeloid cells promotes obesity-induced muscle insulin resistance. EMBO Mol Med 2014; 6: 43–56.

Yeung WL, Lam CW, Hui J, Tong SF, Wu SP. Galactorrhea-a strong clinical clue towards the diagnosis of neurotransmitter disease. Brain Dev 2006; 28: 389–91.

Zhou QY, Palmiter RD. Dopamine-deficient mice are severely hypoactive, adipsic, and aphagic. Cell 1995; 83: 1197–209.

Zhou QY, Quaife CJ, Palmiter RD. Targeted disruption of the tyrosine hydroxylase gene reveals that catecholamines are required for mouse fetal development. Nature 1995; 374: 640–3.

Zigmond RE, Schwarzschild MA, Rittenhouse AR. Acute regulation of tyrosine hydroxylase by nerve activity and by neurotransmitters via phosphorylation. Annu Rev Neurosci 1989; 12: 415–61.